ECMWF Feature article

EARTH SYSTEM SCIENCE

Improving mesoscale aspects in the ensemble forecast initial conditions
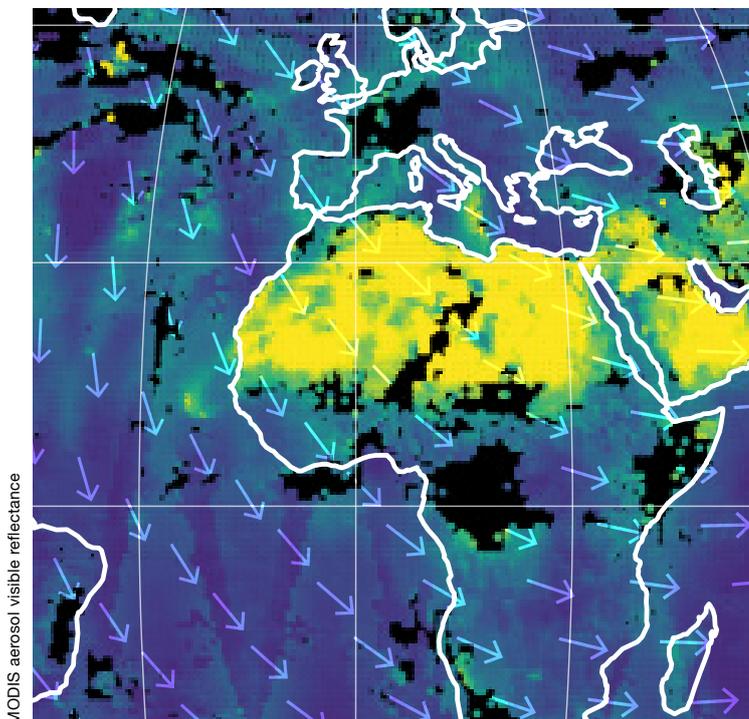
MODIS aerosol visible reflectance

Improving mesoscale aspects in the ensemble forecast initial conditions

Martin Leutbecher, Sarah-Jane Lock, Elias Hólm, Aristofanis Tsiringakis, Marieke Plesske, Ioan Hadade

The increase in horizontal resolution of the Ensemble of Data Assimilations (EDA) from 18 km to 9 km in Cycle 49r1 of the Integrated Forecasting System (IFS) has sharpened the depiction of mesoscale features, enabling better representation of weather phenomena – especially in areas where observational data is sparse. While this has clear benefits, it has also exposed a challenge in how ensemble forecast initial conditions are constructed.

The methodology for constructing ensemble initial conditions involves re-centring the EDA onto the deterministic analysis. However, the re-centring can introduce spurious structures in the smaller scales for individual ensemble members. These artefacts have become more noticeable with the increased mesoscale variability in Cycle 49r1 and are particularly evident for tropical cyclones, which may appear deformed or may have double cores. To address this, a new method has been developed to re-centre the EDA onto the deterministic analysis in a scale-dependent way, improving the realism of the mesoscales in the ensemble initial conditions. This article outlines the motivation for the new approach, explains how scale-dependent re-centring is implemented, and summarises its meteorological impacts and operational integration in Cycle 50r1.

As well as perturbations from the EDA, the ensemble initial conditions include singular vector perturbations. The method for generating these remains unchanged, so we do not discuss them further, but they are nonetheless part of the experiments reported below.

Re-centring of the EDA

The EDA was introduced in 2010 as a method for representing initial uncertainties in ECMWF ensemble forecasts (Buizza et al., 2008). In addition, it plays a key role in estimating situation-dependent background error covariances in variational data assimilation. Each ensemble forecast begins with slightly different initial conditions that reflect possible errors in the analysis. These are constructed by combining the deterministic analysis with perturbations from the EDA. Specifically, the difference between an EDA member and the EDA mean (i.e. an EDA perturbation) is added to the deterministic analysis (see Box, equation 1). The combination of the EDA with the deterministic analysis can be viewed as a shifting, or 're-centring', of the EDA with an increment consisting of the difference between the deterministic analysis and the EDA mean (Box, equation 2).

Re-centring is an important step as perturbed EDA members use a computationally cheaper configuration and are based on observations available six hours earlier than those used in the deterministic analysis (Lang et al., 2015). Aligning the ensemble members with the deterministic analysis therefore increases the probabilistic skill of the ensemble forecasts.

However, this approach has limitations. At the higher resolution in Cycle 49r1, the EDA contains richer mesoscale variability, and the re-centring occasionally produces unrealistic small-scale features in the ensemble initial conditions, in particular for those that are poorly constrained by observations (Lang et al., 2015). The variability in smaller scales in the EDA increased considerably with the horizontal resolution increase to TCo1279 (9 km) in Cycle 49r1 (Roberts et al., 2024).

Scale-dependent re-centring of the EDA

Motivated by work on re-centring perturbed EDA members within the EDA itself (Hólm et al., 2022), the idea emerged to spatially filter the increment used to re-centre the ensemble initial conditions on the deterministic analysis. The filtering operation is implemented in spectral space and applied to the upper-air fields of the increment (Box, equation 3). The filter scales are controlled by specifying a filter wavenumber, *N*. Waves with a total wavenumber larger than *N* (representing the smaller scales) are removed by the filter, while those with a total wavenumber up to and including *N* (representing the larger scales) remain unchanged. In this way, each ensemble member keeps the overall structures from the corresponding EDA member, while only the larger scales are shifted towards the more accurate and more recently updated deterministic state.

Re-centring methodology

Standard re-centring

The initial condition for each ensemble member j is constructed by adding that member's EDA perturbation to the deterministic analysis:

$$x_j = x_c + x_{EDA,j} - \overline{x_{EDA}} \qquad (1)$$

Meaning:

Initial condition = deterministic analysis + deviation of that EDA member from the EDA mean.

See the schematic (a) for an illustration of the terms.

Note, the EDA does not run in the time-critical path, so its analyses are not yet available when the ensemble forecasts are started. Instead, 6-hour EDA forecasts from the most recently available EDA analyses must be used as a proxy.

Figure 1 illustrates examples of x_j for mean sea level pressure. Figure 2 represents x_c, and examples of $x_{EDA,j}$ can be seen in Figure 3. Not illustrated: $\overline{x_{EDA}}$ would be the mean field constructed from all EDA members, $x_{EDA,j}$ (j=1,…, 50).

Scale-dependent re-centring

Equation (1) can be rewritten as:

$$x_j = x_{EDA,j} + x_c - \overline{x_{EDA}} \qquad (2)$$

Here, the increment $x_c - \overline{x_{EDA}}$ shifts the EDA member towards the deterministic analysis.
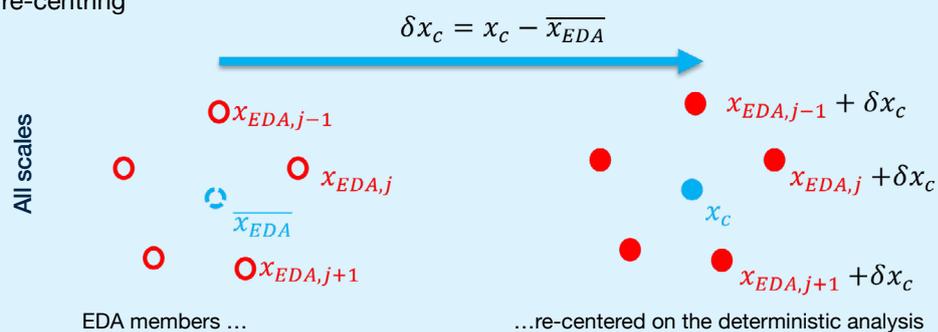
In the new approach, the increment is passed through a spectral filter F_N, so that only large-scale components are retained.
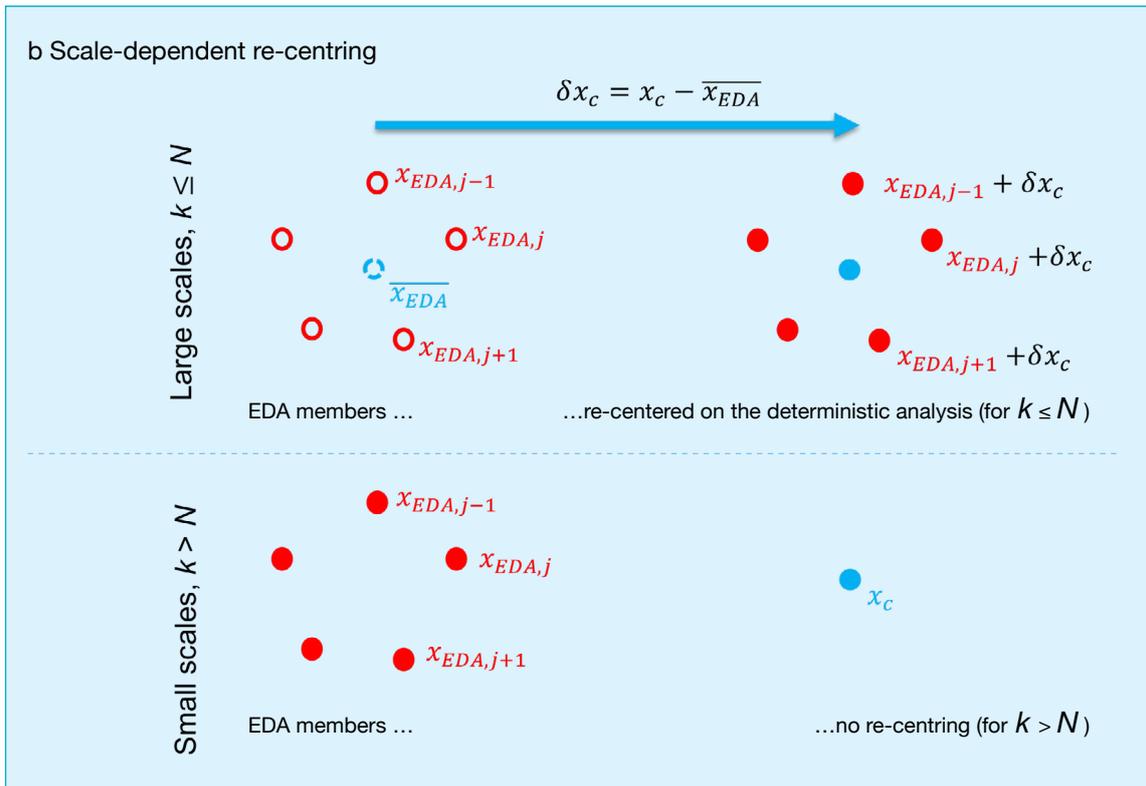
$$x_j = x_{EDA,j} + F_N(x_c - \overline{x_{EDA}}) \qquad (3)$$

Wavenumbers up to N are preserved; higher wavenumbers are removed. This keeps the smaller-scale patterns from the EDA while aligning only broad-scale features with the deterministic analysis.

Figure 4 illustrates examples of x_j for mean sea level pressure, with spectral filter F_N applied for *N=159*.

a Standard re-centring

b Scale-dependent re-centring

$$\delta x_c = x_c - \overline{x_{EDA}}$$

Large scales, $k \leq N$

$x_{EDA,j-1}$
$x_{EDA,j}$
$\overline{x_{EDA}}$
$x_{EDA,j+1}$

$x_{EDA,j-1} + \delta x_c$
$x_{EDA,j} + \delta x_c$
$x_{EDA,j+1} + \delta x_c$

EDA members …   …re-centered on the deterministic analysis (for $k \leq N$)

Small scales, $k > N$

$x_{EDA,j-1}$
$x_{EDA,j}$
$x_{EDA,j+1}$

x_c

EDA members …   …no re-centring (for $k > N$)

Sensitivity tests on the filter wavenumber were carried out to determine the impact on ensemble skill and the occurrence of spurious structures in the ensemble initial conditions.

When *N* is small, spurious structures disappear from the initial conditions. However, when *N* is too small, too little information is retained from the more recent deterministic analysis, leading to degraded ensemble skill compared to using the standard EDA re-centring approach that uses all scales of the increment. Noticeable skill degradations start to emerge for values of *N* of less than about 100. Conversely, when *N* is larger than about 250, significant spurious structures remain, particularly around tropical cyclones. Based on these results, a spectral filter with *N* = 159 was chosen for implementation. This corresponds to waves with a wavelength of about 250 km.

Systematic evaluation of the impact of the revised ensemble initial conditions

The impact of scale-dependent re-centring on ensemble forecasts has been evaluated for a larger sample of cases as is usual for any meteorologically active change that is planned to enter operations. Medium-range ensemble forecast experiments have been run for two periods at operational resolution (TCo1279, approx. 9 km): June–August 2022 (85 cases) and December 2022–February 2023 (83 cases). These experiments included ten perturbed members, initialised from analyses and an EDA at the same resolution. The introduction of the scale-dependent re-centring (*N* = 159) leads to a small increase in mean tropical cyclone core pressure of about 1–2 hPa which quickly decreases with forecast lead time. In terms of root mean square (RMS) error of the ensemble mean, the impact on core pressure is neutral. The revision of the ensemble initial conditions does not lead to a statistically significant change in the error of the ensemble mean position of tropical cyclones beyond initial time. The spread in the tropical cyclone position shows a moderate increase in the boreal summer period at lead times up to four days, while no change is observed in the boreal winter period.

The medium-range ensemble forecasts have also been used to quantify the impact of the scale-dependent re-centring for probabilistic skill of the ensemble. Figure 5 shows the fair Continuous Ranked Probability Score (fCRPS) of 500 hPa geopotential for the period June–August 2022 (92 start dates). Relative improvements in fCRPS were small (<0.5%) and consistent with slightly increased spread (not shown), at early lead times. Overall, the impact on probabilistic skill is very close to neutral.

case study | Tropical Cyclone Freddy

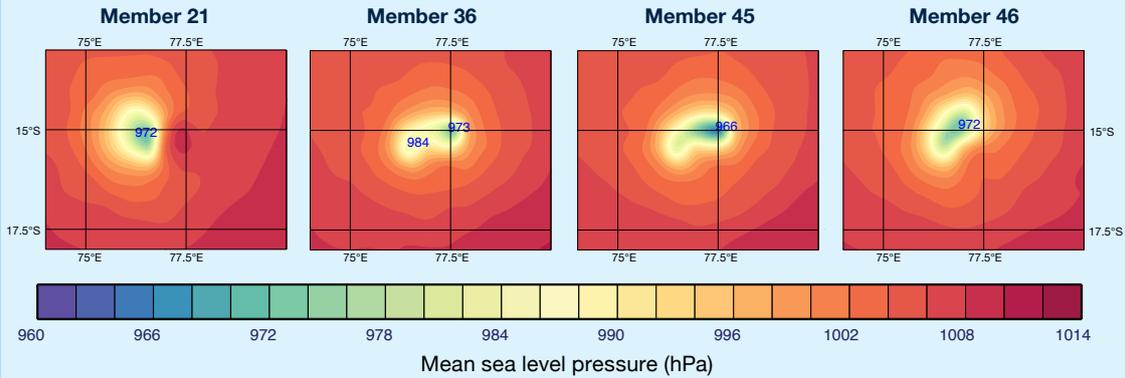**Member 21** | **Member 36** | **Member 45** | **Member 46**

FIGURE 1 Mean sea level pressure (hPa) of the initial conditions for Tropical Cyclone Freddy (valid 17 February 2023, 00 UTC) of four ensemble members constructed with the standard EDA re-centring operational in Cycle 49r1. Members display unrealistic structures such as distorted or double-centre vortices.

The benefits of scale-dependent re-centring of the EDA are particularly evident in the ensemble initial conditions for tropical cyclones.

Tropical Cyclone Freddy was an intense and long-lasting tropical cyclone that tracked westward across the Indian Ocean in February 2023, passing north of La Réunion and later making landfall in Madagascar and Mozambique. Using the standard re-centring in Cycle 49r1, some ensemble members display distorted, elongated or double-core vortex patterns. Examples of ensemble members with artefacts in the initial conditions are shown in Figure 1:

- Member 21 has an anticyclonic anomaly located east of the centre of the cyclone leading to a zone of enhanced pressure gradients and anomalously large curvature of the isobars in the SE quadrant of the storm.

- Member 36 has a double centre and is elongated in the zonal direction.

- Member 45 is also elongated in the zonal direction with a hook-shaped appearance and anomalous curvature of the isobars south of the centre.
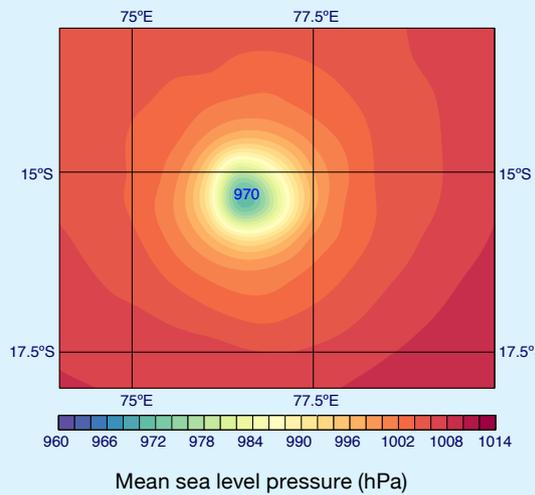

FIGURE 2 Mean sea level pressure (hPa) of the deterministic analysis for Tropical Cyclone Freddy (valid 17 February 2023, 00 UTC).

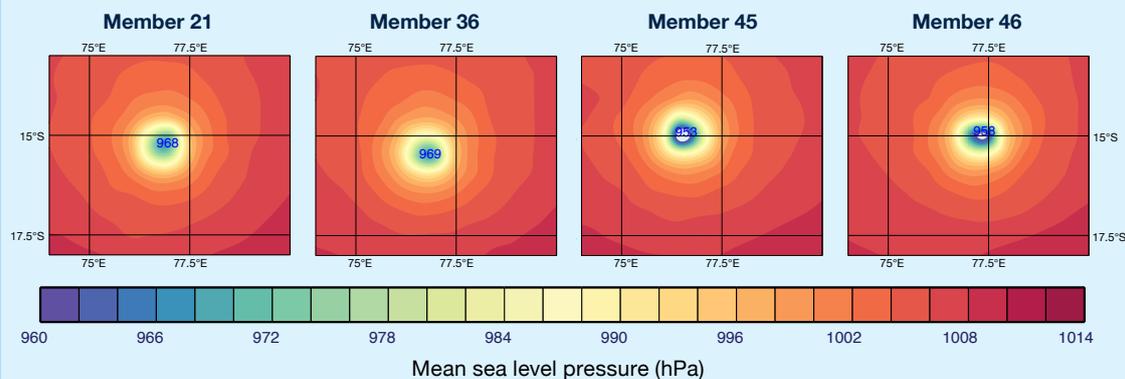**Member 21** | **Member 36** | **Member 45** | **Member 46**

FIGURE 3 Mean sea level pressure (hPa) of 6-hour forecasts from EDA members 21, 36, 45 and 46 for Tropical Cyclone Freddy (valid 17 February 2023, 00 UTC).
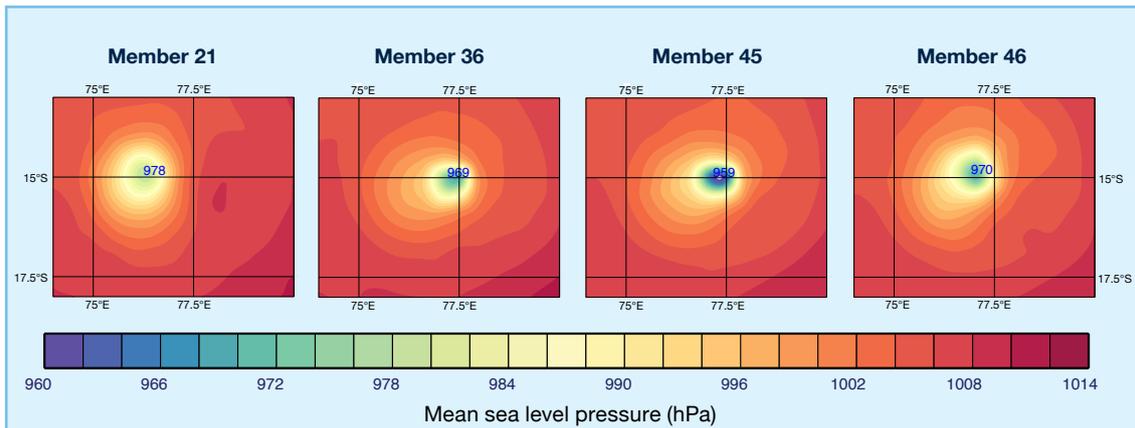
FIGURE 4 Mean sea level pressure (hPa) of the initial conditions for Tropical Cyclone Freddy (valid 17 February 2023, 00 UTC) of four ensemble members constructed with the scale-dependent EDA re-centring that will be operational in Cycle 50r1. The unrealistic vortex distortions seen in Figure 1 are no longer present.

- Member 46 is elongated in the south-west to north-east direction and has anomalously curved isobars on the south-east side.

These unrealistic structures were absent in the deterministic analysis and the EDA members used for constructing the initial conditions (Figures 2 and 3). Importantly, these structures disappear during the first 24 hours of the forecast, which is consistent with them being artefacts of the re-centring process rather than real atmospheric phenomena.

When scale-dependent re-centring of the EDA was applied ($N = 159$), all four members showed much more axisymmetric, realistic cyclone structures (Figure 4).

Across the 50-member ensemble for this case, roughly a third of the members showed major deviations from axisymmetry in the Cycle 49r1 initial conditions, but none exhibited major deformations when applying the spectral filter to the increment.

Atmospheric winds exhibit variability that depends on the spatial scales and this can be quantified by looking at kinetic energy spectra. These show variances of wind anomalies as a function of wavenumber (i.e. inverse wavelength). With standard re-centring, the variance at initial time is considerably larger (up to 75% more) than at later lead times for all wavenumbers exceeding 50 (Figure 6). Most of the excess variance in the small scales dissipates relatively quickly during the first day of the forecast. In contrast, forecasts starting from initial conditions obtained with the scale-dependent EDA re-centring (with $N = 159$) exhibit large excess variance only in a band of wavenumbers between 50 and 160.

Implementation in operations

The construction of the ensemble initial conditions depends on the availability of the deterministic analysis and is therefore time critical. With the scale-dependent EDA re-centring, additional time is
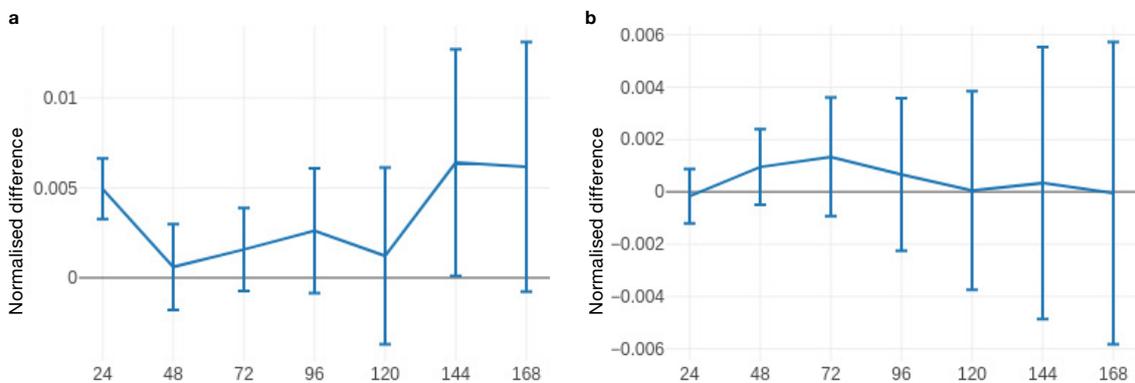

FIGURE 5 Relative change in fair Continuous Ranked Probability Score (fCRPS) versus lead time (hours) for 500 hPa geopotential in (a) the northern extratropics and (b) the southern extratropics during the period June–August 2022. Positive values imply higher skill for the experiment with scale-dependent re-centring of the EDA. Vertical bars are confidence intervals at the 99.7% level.
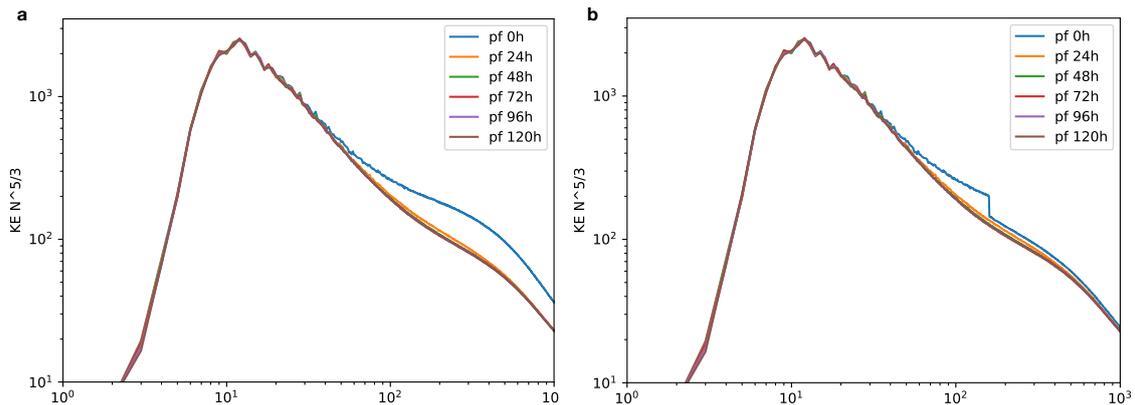
FIGURE 6 Kinetic energy spectra for 250 hPa wind anomalies for (a) an ensemble with initial conditions as in Cycle 49r1 and (b) an ensemble with initial conditions using the scale-dependent EDA re-centring. Curves correspond to lead times from 0 to 120 hours. The kinetic energy is scaled so that a -5/3 spectrum would appear as a flat line. Data are aggregated for June 2022 and all ten perturbed members. Anomalies are computed with respect to the monthly mean wind.

required for the new tasks that perform the spectral filtering. Without attention, this would have reduced the available time for running the ensemble forecast in the operational schedule. However, the additional time has been absorbed by other optimisations in the auxiliary code that is used to construct the ensemble initial conditions – optimisation work that has considerably eased the implementation of scale-dependent re-centring in Cycle 50r1.

Conclusion

The resolution upgrade of the EDA to TCo1279 (9 km) in Cycle 49r1 has exposed known limitations in the generation of ensemble forecast initial conditions. These manifest themselves in spurious mesoscale structures that can be seen for instance around tropical cyclones or in excess small-scale variance at initial time. Scale-dependent re-centring of the EDA on the deterministic analysis addresses these deficiencies in the mesoscale. Results from a case study for Tropical Cyclone Freddy in 2023 illustrate the marked improvement in the realism of the initial conditions and broader evaluation shows minimal impact on the probabilistic skill. The method also integrates efficiently into the operational schedule, facilitating its implementation in Cycle 50r1.

This development illustrates the continuous evolution of ensemble forecasting techniques, ensuring that higher-resolution data translates into more realistic, reliable forecasts without compromising integrity. As the EDA advances (e.g. if it could be run in real time and therefore have seen the latest observations), it might be possible to allow even more selective re-centring, further improving mesoscale realism while preserving ensemble forecast skill.

Further reading

Buizza, R., **M. Leutbecher & L. Isaksen.**, 2008: Potential use of an ensemble of analyses in the ECMWF Ensemble Prediction System. *Q. J. R. Meteor. Soc.,* **134**, 2051–2066. *https://doi.org/10.1002/qj.346*

Hólm, E., **M. Bonavita**, & **S. Lang**, 2022: Soft recentring Ensemble of Data Assimilations. *ECMWF Newsletter* **No. 171**.

Lang, S. T. K., **M. Bonavita** & **M. Leutbecher**, 2015: On the impact of re-centring initial conditions for ensemble forecasts.
Q. J. R. Meteor. Soc., **141**, 2571–2581. *https://doi.org/10.1002/qj.2543*

Roberts, C., **B. Ingleby**, **A. Geer**, **E. Hólm**, **M. Janousek**, **F. Prates** & **M. Rodwell**, 2024: IFS upgrade improves near-surface wind and temperature forecasts. *ECMWF Newsletter* **No. 181**, 16–25. *https://doi.org/10.21957/crx2bn4is8*